Critical Driving Forces for Formation of Bainite

LINDSAY LEACH, PETER KOLMSKOG, LARS HÖGLUND, MATS HILLERT, and ANNIKA BORGENSTAM

An empirical equation for predicting bainite start temperatures of steels was recently derived by starting from binary Fe-C alloys and continuing with ternary Fe-C-M alloys. This result is now illustrated with a family of B_S lines in a *T,C* diagram for a series of constant Mn contents. The critical driving force for the formation of ferrite is calculated for diffusionless or diffusional processes, and these quantities are used as dependent variables with carbon content or temperature as independent variables. Negative critical driving forces are predicted for a diffusionless process in binary Fe-C alloys, showing that this process cannot apply to the formation of bainite. The critical driving force for a diffusional process increases strongly with decreasing temperature and increasing carbon content. Mn and Ni, contrary to Cr, Mo and Si, have remarkably small effects on this critical driving force. The results are discussed by imagining that the magnitude of the critical driving force is governed by the height of an energy barrier that must be surmounted during growth. It is modeled as completely determined by the alloy composition. It is represented with an equation evaluated by fitting to the recent empirical equation and describing the carbon dependence of the barrier.

https://doi.org/10.1007/s11661-018-4819-5

I. INTRODUCTION

BAINITE is a microstructure that often forms in steels on cooling of the high-temperature phase, austenite. It can give the steel very useful properties, and there has long been a need to predict the bainite start temperature, B_S, from the composition. For Fe-C alloys one may represent the critical conditions of bainite formation from austenite with the B_S line in a *T,C* diagram. Usually B_S is described as the critical temperature of bainite formation for a fixed carbon content but could as well represent the same B_S as the critical carbon content at a fixed temperature. There are thus two natural ways of representing the B_S function, $B_S = T_{crit}(C)$ or $B_S = C_{crit}(T)$. To distinguish between these two functions, they can be denoted as $B_S(T_{crit})$ and $B_S(C_{crit})$. Mathematically, they may look very different but they represent the same B_S line in the *T,C* diagram.

For any point in the *T,C* diagram, many thermodynamic properties can be calculated from a thermodynamic database, always obtaining a unique value, *e.g.*, the thermodynamic driving force for the transformation, and it is well known that bainite does not start to form until there is a substantial driving force. From experimental information on the B_S line in a *T,C* diagram, one can thus calculate the critical driving force, DF_{crit}, and evaluate a function $DF_{crit}(T)$ for an Fe-C alloy under the condition that the alloy is situated on the B_S line. Then, a B_S line can be plotted in a *DF,T* diagram, which represents the same critical conditions as the B_S line in the *T,C* diagram. The function representing the B_S line in this diagram will also be denoted as B_S but it will be given as $B_S = DF_{crit}(T)$ or $B_S = T_{crit}(DF)$. This is again a case where two B_S functions may look very different mathematically but actually represent the same B_S line in a diagram. One could also define $DF_{crit}(C)$ or $B_S = C_{crit}(DF)$. All these functions and corresponding diagrams with B_S lines can also be constructed for any fixed alloy content in a steel. The aim of the present work was to explore the usefulness of this kind of diagram by plotting the same B_S lines in these different ways.

Many equations of B_S temperatures have been proposed,[1–10] *e.g.*, an early one by Steven and Haynes,[1] in which the coefficients for carbon and alloying elements were determined by linear regression analysis of experimental B_S information from a group of 65 steels, mainly commercial ones. In these equations it is assumed that the effects of alloying elements are independent of carbon content, which will here have the symbol *C*, irrespective of in what unit it is expressed. For binary Fe-C alloys with different carbon contents, one can

LINDSAY LEACH, LARS HÖGLUND, MATS HILLERT, and ANNIKA BORGENSTAM are with the Department of Materials Science and Engineering, KTH Royal Institute of Technology, Brinellvägen 23, 10044 Stockholm, Sweden. Contact e-mail: lindsayl@kth.se PETER KOLMSKOG is with Sandvik Mining and Rock Technology, Sandvik Industrial Area, 6480-RTDRB, 811 81 Sandviken, Sweden.

Manuscript submitted March 21, 2018.
Article published online July 27, 2018

represent experimental B_S information by a B_S line in the T,C diagram. In this connection, B_S is identical to the critical temperature for bainite formation as a function of the carbon content, $T_{crit}(C)$, and that is how it used for measurement. The dependence on alloying elements was thus represented by equations of the following form by choosing a simple linear equation,

$$B_S \equiv T_{crit}(C, M) = a - bC - \sum k_i M_i, \qquad [1]$$

M represents the contents of all the alloying elements present. This is the form used by Steven and Haynes, and the following equation is a recent example[11] of the same form but was derived by first evaluating the a and b coefficients from binary Fe-C information and then the k_i coefficients one by one from the respective ternary information.

$$\begin{aligned} WB_S &\equiv T_{crit}(C, M) \\ &= 850 - 206C - 78Mn - 33Ni - 70Cr - 75Mo \\ &\quad - 61Si. \end{aligned} \qquad [2]$$

This will be regarded as an empirical equation because the coefficients have been evaluated from experimental information and not from some model. From the upper part of the temperature range it was based on information from Widmanstätten ferrite, and the notation B_S was thus changed to WB_S. This symbol will be used in the present work when information from Widmanstätten ferrite is involved. As an example, Figure 1 shows the family of WB_S lines, calculated from Eq. [2] for a series of Mn contents. The WB_S line for binary Fe-C alloys is denoted as WB_S^o.

From a linear equation like Eq. [2] one can define a WB_S line for any set of alloys with equal alloy content but different carbon contents. It should be emphasized that access to an analytical representation of experimental information, such as Eq. [2], was important in the present work, which is based on illustrations with WB_S lines. Experimental values are not close enough to be applied directly and always show some scatter, which makes diagrams more difficult to interpret. Equation [2] was chosen as the most reliable empirical equation to represent the experimental information because it was evaluated primarily from binary Fe-C information, which must be used as the reference for expressing effects of alloying elements. Values calculated from Eq. [2] will be regarded as empirical to be distinguished from values obtained by modeling. The four filled circles in Figure 1 are empirical points, calculated for Fe-C alloys from Eq. [2], and fall on the WB_S^o line, which was calculated from the same equation. The four crosses apply to the same Fe-C alloys but were calculated from a model, and it is evident that it is not consistent with the empirical Eq. [2].

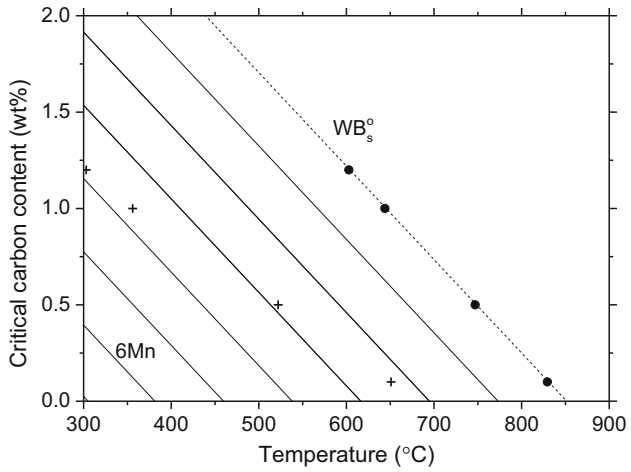

Fig. 1—Empirical WB_s temperatures plotted for critical carbon contents in Fe-C-Mn alloys. The dashed line, WB_s^o, is for Fe-C alloys, and the filled circles on it are WB_s^o temperatures for alloys with 0.1, 0.5, 1.0 and 1.2 wt pct carbon. The four crosses are for the same alloys but are obtained by modeling. Both groups will be discussed later.

The carbon content in Figure 1 is stated as critical to emphasize the possibility of studying the critical condition of bainite formation through the critical carbon content. Hillert[12] explored this possibility by extrapolating the lengthening rate of acicular ferrite at constant temperature to zero for a series of plain carbon steels of various carbon contents to find the critical carbon content. His primary aim was to evaluate the distance of the critical carbon content from the A_3 line to calculate the critical driving force for the formation of acicular ferrite in Fe-C alloys by assuming a diffusional growth process. It will here be denoted as DFD_{crit}, where the second D stands for diffusion. He could then plot his results in two ways, in the usual T,C diagram and in a T, DFD diagram. He regarded both lines as expressions of the same critical condition and used the same symbol in both diagrams. He chose WB_S to emphasize that the critical condition was experimentally determined from B_S for bainitic ferrite at lower temperatures and from W_S for Widmanstätten ferrite at higher temperatures. He supported the use of the common symbol, WB_S, by reporting that he did not observe any kinetic difference between the low and high temperature ranges. Independent of the axis variables, Hillert thus applied this symbol for the critical condition where bainite starts or stops forming and this procedure was accepted in the present work.

Hillert *et al.*[13] later derived the same kind of WB_S line, expressed through a critical driving force, but it was then evaluated from W_S or B_S values of only two Fe-C alloys and one Fe-C-Si alloy in the hope that Si would have a negligible effect. They described the $DFD_{crit}(T)$ function with a spline function and tested it on steels with one alloying element at a time under the assumption that there would be no effect of alloying elements in addition to their thermodynamic effect on the calculation of driving force. They could reproduce experimental B_S temperatures for Mn and Ni with some success, which seemed to indicate that DFD_{crit} is rather independent of those elements but there was no success for Cr or Mo.

In the meantime, Bhadeshia[14] had evaluated the same driving force from B_S temperatures of steels

studied by Steven and Haynes,[1] from which they derived their empirical equation for predicting B_S temperatures. However, he proposed that this driving force would apply only to the formation of Widmanstätten ferrite. From the same B_S information, Bhadeshia also evaluated the critical driving force for a diffusionless transformation of austenite to ferrite, and it is evident that he did not include Widmanstätten ferrite in that analysis. It will here be denoted as DFN_{crit} where N stands for no diffusion. From some results he proposed that this critical driving force should be 400 J/mol independent of alloying additions. There have thus been two proposals based on the idea that the critical condition of bainite formation can be expressed through a $DF_{crit}(T)$ function for a diffusional or diffusionless process. The diffusionless and diffusional formation mechanisms of bainite formation may be regarded as two extreme cases, and their feasibility from a thermodynamic point of view will now be examined by studying their driving forces in the hope of finding some clue to what is governing the critical condition of bainite formation. The study will be based on the experimental information summarized by Eq. [2].

II. CALCULATION OF DRIVING FORCES

It is common procedure to represent the deviation from local equilibrium at a moving phase interface with a thermodynamic driving force. Sometimes it is presumed that this driving force surmounts a physical barrier to the movement when it has reached the same magnitude at a critical temperature. The present work is limited to the thermodynamic aspects and the term energy barrier will be used as a synonym to driving force when this special aspect is emphasized but without a particular physical interpretation of the barrier. The driving force for a diffusionless formation of ferrite from austenite is obtained as

$$DFN = G^{\gamma}_{m}(T, C, M) - G^{\alpha}_{m}(T, C, M), \qquad [3]$$

where both C and M have the same value in the two phases. For a fixed alloying content, M_1, there are only two independent variables,

$$DFN = G^{\gamma}_{m}(T, C) - G^{\alpha}_{m}(T, C). \qquad [4]$$

When evaluating the critical driving force for the start of bainite formation one must introduce the relation between C and T, which is defined by the B_S line in the T,C diagram. Then, there will be only one independent variable.

$$DFN_{crit}(TorC) = G^{\gamma}_{m}(TorC) - G^{\alpha}_{m}(TorC). \qquad [5]$$

From a WB_S line in a T,C diagram one may thus calculate DFN_{crit} in any T,C point on the the B_S line and plot the WB_S line in a T,DFN diagram or a C,DFN diagram.

For diffusional growth of bainitic ferrite from austenite, Hultgren[15] proposed that there is no change of the contents of alloy elements from austenite to ferrite. This should hold for all substitutional elements but only if the contents are expressed in a mole fraction related to the ordinary mole fraction by $u_j \equiv x_j / \sum_S x_i = x_j/(1 - x_C)$. The criterion is thus written as $u^{\alpha}_j = u^{\gamma}_j$ for all substitutional elements, S, which also includes Fe. This mole fraction must be used here because the ordinary mole fractions, x_i, will vary with the carbon contents of the phases. Under this condition, all these elements behave as one, and local equilibrium of this component and of carbon at the phase interface yields

$$\sum_S u^{\gamma}_j \mu^{\gamma}_j = \sum_S u^{\alpha}_j \mu^{\alpha}_j = \sum_S u^{\gamma}_j \mu^{\alpha}_j, \qquad [6]$$

$$\mu^{\gamma}_C = \mu^{\alpha}_C. \qquad [7]$$

For the interstitially dissolved carbon, Hultgren proposed that there is full equilibrium across the interface. Hultgren called this situation paraequilibrium. However, the interface can move only if there is a driving force acting on it. This requires a deviation from equilibrium across the interface but should only apply to the substitutional atoms. This deviation can be evaluated as a driving force.

$$DFD = \sum_S u^{\gamma}_j \mu^{\gamma}_j - \sum_S u^{\gamma}_j \mu^{\alpha}_j = \sum_S u^{\gamma}_j \left(\mu^{\gamma}_j - \mu^{\alpha}_j\right) \qquad [8]$$

To avoid misunderstandings, it is now proposed that this growth condition of bainitic ferrite be called a paracondition because the driving force represents a deviation from equilibrium. The effect of the carbon contents of the two phases on Eq. [8] is not immediately evident since it is indirect through the effects on the respective chemical potential. For this kind of driving force there are two carbon contents, C^{α} and C^{γ}, but one more condition due to Eq. [7]. Both will be evaluated in the following calculations but C^{α} will not be shown. The notation C will refer to the carbon content of austenite, C^{γ}, which is also the carbon content of the alloy.

The present work depends on thermodynamic information and computer software. Calculations were performed with the Thermo-Calc software[16] and the TCFE8 database.[17] For a special case, a database developed by Bhadeshia[18] was also applied. That database is available on the internet together with adequate software by Peet and Bhadeshia.[19]

III. CRITICAL DRIVING FORCE FOR DIFFUSIONLESS PROCESS

As already explained, any point in Figure 1 gives the critical carbon content of austenite for bainite formation at the selected temperature and Mn content. The system is thus completely defined and using a thermodynamic database one can in principle define and calculate the value of any thermodynamic property of austenite with this composition. The critical driving force for

diffusionless formation of ferrite is one such property, and the result is plotted in Figure 2. Following the examples of Hillert[12] and Bhadeshia[14] for driving forces, temperature was used as the independent variable but lines for a series of constant carbon contents were added as dash-dot lines. The WB_S lines for a series of Mn contents represent the same critical states as in Figure 1 but now plotted with a different pair of variables. Any point in Figure 2 will thus give the complete composition of an alloy with the given critical driving force. The four points on the WB_S^o line in Figure 1 hold for binary Fe-C alloys with 0.1, 0.5, 1.0 or 1.2 mass pct carbon, and in Figure 2 they again fall on the WB_S^o line. All the parallel lines for constant Mn contents should still be identified as the family of WB_S lines from Figure 1. These lines are described by the following functions, $WB_S^o \equiv DFN_{crit}(T, 0)$ and $WB_S \equiv DFN_{crit}(T, M)$, respectively. The similarity between Figures 1 and 2 would be more striking by imagining a family of horizontal lines for constant carbon contents in Figure 1. Both would then have two families of intersecting lines representing the manganese and carbon content.

As already mentioned, Bhadeshia[14] proposed that growth of bainitic ferrite occurs without diffusion of carbon. He denoted the corresponding driving force by-*FTO,* which has here been denoted as *DFN*. Empirical information on the critical values of this quantity was already presented in Figure 2 as the solid lines for a number of fixed Mn contents and as dash-dot lines for a number of carbon contents. For each point in the diagram, *i.e.*, for each alloy with fixed Mn and C content, one can read the critical temperature on the abscissa. In an effort to examine whether the diffusionless proposal can be applied to binary Fe-C alloys, the driving force, *i.e.*, *DFN* or-*FTO*, was then calculated in a range of temperatures for the four Fe-C alloys represented by the circles in Figures 1 and 2, where they are only shown at their critical temperatures. For the sake of consistency, these calculations were performed with Bhadeshia's own database and software.[18] The result is presented in Figure 3, and the crosses in the intersections with the horizontal line for 400 J/mol show under what conditions bainite could start forming according to Bhadeshia's model. The critical temperature is again found on the abscissa. The crosses thus represent the model-predicted B_S^o conditions of these four binary alloys and should be compared with the empirical B_S^o information of these binary alloys, represented by the four circles on the WB_S^o line in Figure 1. This empirical information was already transferred to a diagram with a DFN_{crit} axis in Figure 2 and was then transferred to Figure 3, where it ideally should have fallen on the extensions of the curves for the same alloys. However, those curves were calculated with software from Peet and Bhadeshia,[19] which stopped automatically when the driving force turned negative. The curves were thus connected to the empirical points by hand. It should be emphasized that the curves in Figure 3 were calculated with the database from Bhadeshia,[18] which fact is indicated by the use of his symbol-*FT0* for the driving force of a diffusionless process. The four points were calculated from the database defined by Eq. [2]. The extrapolations look reasonable, which indicates that the two databases are rather similar.

The distance between the sets of model-predicted crosses and empirical circles in Figure 3 is very large. It was thus concluded that bainitic ferrite does not form in a diffusionless fashion in binary Fe-C alloys. This is further demonstrated by the fact that the empirical information falls within the negative range of driving force, which by itself demonstrates that bainitic ferrite cannot grow in a diffusionless fashion.

Moreover, the model-predicted B_S^o temperatures in Figure 3 could be directly plotted as crosses in Figure 1 because both the temperature and carbon content were available. There they again illustrate the large difference between the model prediction and empirical information although the negative driving forces were not revealed there.

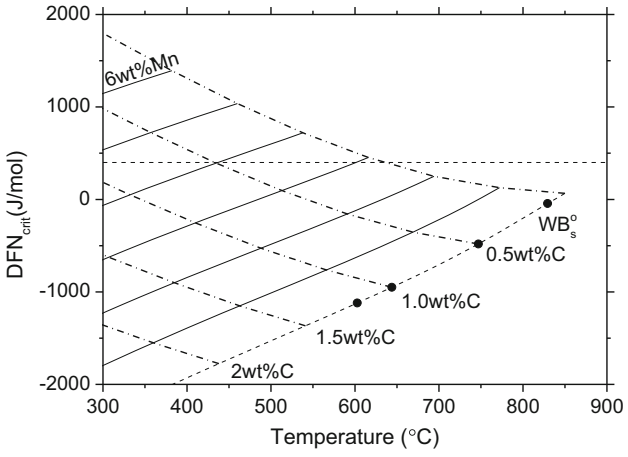

Fig. 2—Critical driving force for the diffusionless process calculated with TCFE8.[17] The solid lines are WB_S lines for various Mn contents. Dash-dot lines are for various carbon contents.

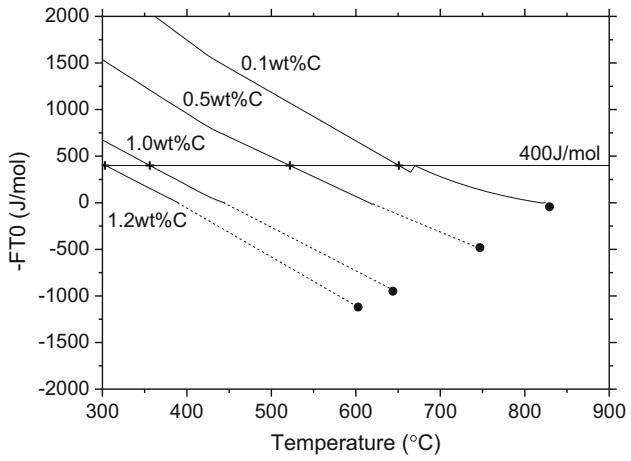

Fig. 3—Driving force for the diffusionless process in four Fe-C alloys. The solid lines are calculated with Bhadeshia's database[18] and are extrapolated with dashed lines to the filled circles, where they intersect the WB_S^o line according to Eq. [2].

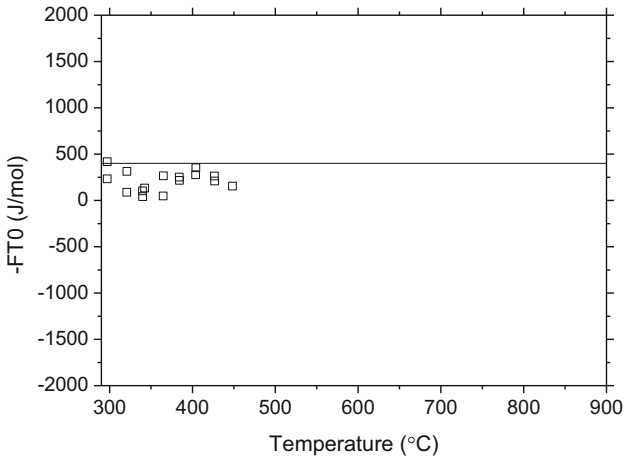

Fig. 4—Temperature dependence of critical driving force for diffusionless process in alloys with fixed Mn and Si contents[20] calculated with Bhadeshia's database.[18]

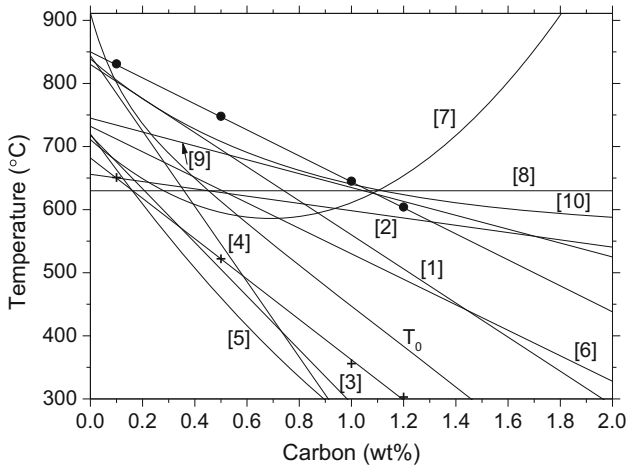

Fig. 5—Various empirical B_S^o lines obtained for Fe-C alloys compared with the T_0 line.

It must be emphasized that the crosses represent predictions for binary Fe-C alloys, and in Figure 1 they should only be compared with the points on the WB_S^o line, which is the only binary part of Figure 1. The observation that the crosses fall among WB_S lines for appreciable Mn contents may provide the following explanation of the large difference. Bhadeshia had proposed that the critical driving force for a diffusionless process should be about 400 J/mol independent of the alloy content, which would seem reasonable from his model of transformation stresses.[13] He tested his proposal by comparison with experimental information from alloys with 3 Mn and 2.12 Si (mass pct). Experimental temperatures and carbon contents were then taken from Reference 20, and the driving force was calculated with the software by Peet and Bhadeshia.[19] The results are presented in Figure 4, which illustrates that the values are rather independent of temperature and rather close to 400 J/mol in an apparent confirmation of the proposed role of a diffusionless process. This result is closely related to the fact that the crosses in Figure 1 fall in a region of considerable Mn contents and there would have been reasonable agreement with empirical information if the crosses had come from an alloy with about 3 mass pct Mn.

Before discarding the diffusionless process for the formation of bainitic ferrite in binary Fe-C alloys, one should consider the possibility that the empirical Eq. [2] is not realistic for binary Fe-C alloys. Actually, there is a wide range of proposals for empirical equations for the B_S^o temperatures, and they can all be used for empirical predictions of the B_S^o line of binary Fe-C alloys. These predictions are illustrated in Figure 5, which is reproduced from Reference 11, but the T_0 line for $DFN = 0$, the WB_S^o line with four circles from Eq. [2] and a line drawn through the four crosses in Figure 1 have been added. Only three of the B_S^o lines fall mainly below the T_0 line and could support the diffusionless reaction for which the line with crosses was calculated. The diffusionless reaction is thus inconsistent with a great majority of the empirically predicted B_S^o lines. The vast difference between the predicted B_S^o line binary Fe-C alloys may mainly be caused by the empirical equations being based on extrapolation from different selections of alloy steels.

The wide variety of proposals, illustrated in Figure 5, may depend on the authors' interest in different kinds of steels. Supposedly, each of the empirical equations may be adequate for predictions in its special range of steel compositions but the values of the coefficients for individual alloying elements are not physically meaningful if the coefficients for carbon are not reasonable for binary Fe-C alloys. As already mentioned, Eq. [2] was derived with special attention to information on binary Fe-C alloys. Even though that information is very meager, it seems that it could not be discarded in favor of the B_S^o line predicted from the diffusionless approach but new information on binary Fe-C alloys is badly needed. From the above discussion it may thus be concluded that a completely diffusionless process is not governing the formation of bainitic ferrite in Fe-C alloys. In any case, if the diffusionless approach is not accepted for binary Fe-C alloys it could hardly be accepted for alloy steels. It seems safe to generalize to alloy steels because it is difficult to imagine that the main characteristics of bainite in binary Fe-C alloys should not apply to bainite in alloy steels. It should be emphasized that to obtain a positive driving force it seems necessary to accept some escape of carbon from the moving phase interface.

IV. CRITICAL DRIVING FORCE FOR DIFFUSIONAL PROCESS

As mentioned in the introduction, Hillert [12] calculated the critical driving force for a diffusional process, DFD_{crit}, from critical carbon contents obtained from growth rate measurements on a series of plain carbon steels. It was further mentioned that Bhadeshia[14] made the same kind of calculation from the B_S information presented by Steven and Haynes[1] and represented the

critical driving force with a straight line rather similar to the corresponding line obtained by Hillert[12] for his series of plain carbon steels. The DFD_{crit} quantity was then calculated for 602 previously used values in the test of Eq. [2],[11] and the result is presented in Figure 6. It shows considerable scatter but strong variation with temperature as in previous studies. Accepting the large scatter, one could fit a straight line to this information, similar to Bhadeshia's line, except for the information above 973 K (700 °C). It is evident that a straight line representation would miss an important feature in the high temperature range of Widmanstätten ferrite.

The $WB_S^o \equiv DFD_{\text{crit}}(T, 0)$ function for binary Fe-C alloys was included in Figure 6 and indicates that the empirical information is strongly asymmetrical. Since practically all the information originates from alloy steels, it is evident that the alloying elements have increased the critical driving force for a diffusional process. This was further explored by calculating the critical driving force for ternary Fe-C alloys with Mn, Ni, Cr, Mo or Si from the empirical Eq. [2], which had already been chosen to represent the empirical B_S information in Reference 11. The $WB_S \equiv DFD_{\text{crit}}(T, M_i)$ function was thus calculated for a series of alloy contents and is presented in Figures 7, 8, 9, 10, and 11, and the $WB_S^o \equiv DFD_{\text{crit}}(T, 0)$ line for binary Fe-C alloys is shown as a dashed curve in all five diagrams. Notably, all the curves in Figures 7, 8, 9, 10, and 11 end inside the diagram when the carbon content, being a dependent variable here, approaches zero. An intersecting family of lines for constant carbon contents could have been included to make these figures similar to Figure 2, and the line for zero carbon would have connected the end points. However, a family of intersecting lines of constant values for an additional dependent variable will be included only for special purposes.

Figures 7, 8, 9, 10, and 11 demonstrate a drastic difference between the effects of alloying elements. Mn in Figure 7 has a very small effect but the magnified

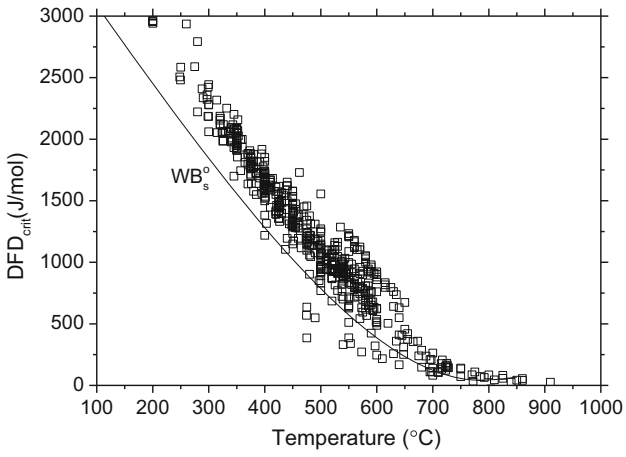

Fig. 6—Critical driving force for a diffusional process in alloys of various composition.

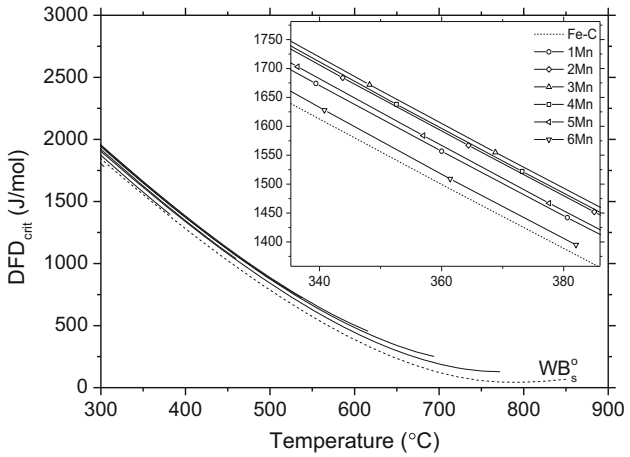

Fig. 7—Critical driving force for a diffusional process as a function of temperature in the Fe-C-Mn system. The dashed line is WB_S^o for Fe-C. The insert shows an increase in driving force until 3 wt pct Mn followed by a decrease to 6 wt pct Mn.

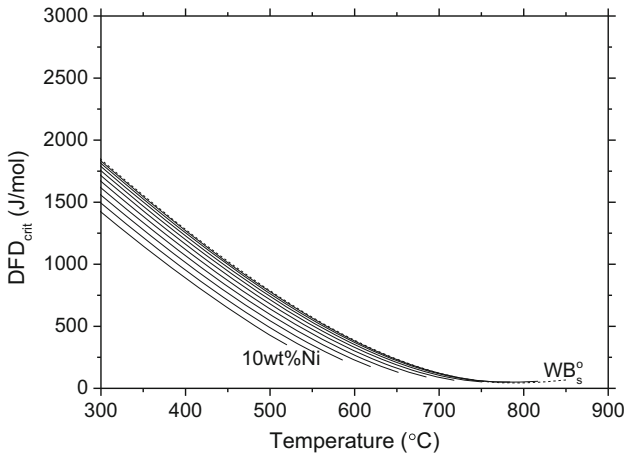

Fig. 8—Critical driving force for a diffusional process as a function of temperature in the Fe-C-Ni system. The dashed line is WB_S^o for Fe-C from which the driving force decreases with addition of Ni.

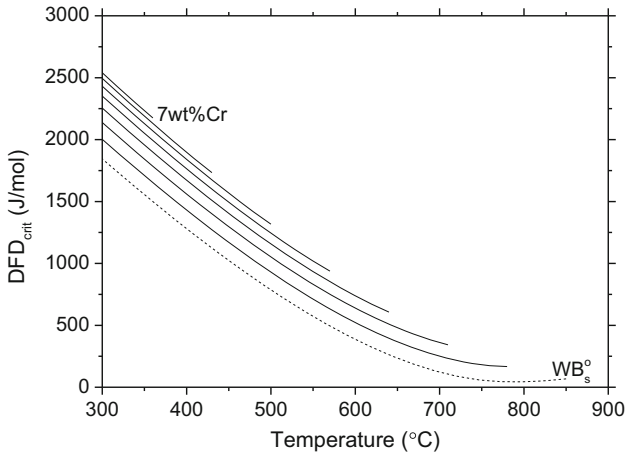

Fig. 9—Critical driving force for a diffusional process as a function of temperature in the Fe-C-Cr system. The dashed line is WB_S^o for Fe-C, and the driving force increases from WB_S^o with addition of Cr.

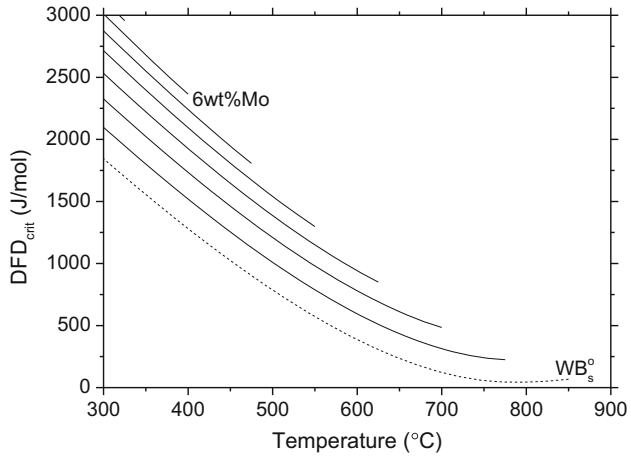

Fig. 10—Critical driving force for a diffusional process as a function of temperature in the Fe-C-Mo system. The dashed line is WB^o_S for Fe-C, and the driving force increases from WB^o_s with addition of Mo.

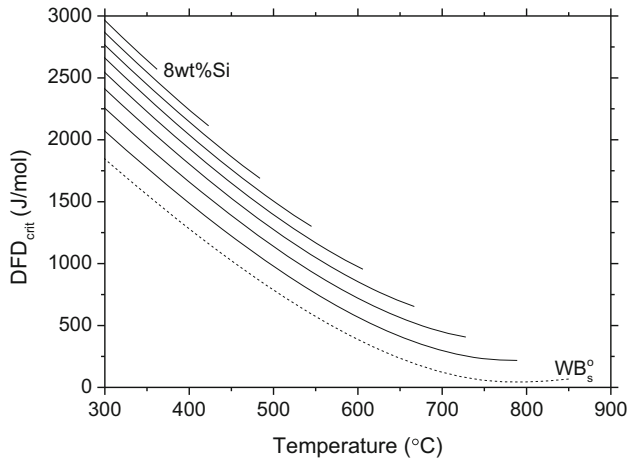

Fig. 11—Critical driving force for a diffusional process as a function of temperature in the Fe-C-Si system. The dashed line is WB^o_S for Fe-C, and the driving force increases with addition of Si.

insert illustrates that it first increases the driving force slightly and the effect is then reversed. In Figure 8, Ni immediately starts to decrease this critical driving force but initially very slowly. The effect accelerates at higher contents. As already mentioned, the small effect of these two alloying elements was observed by Hillert *et al.*,[13] and it inspired them to try to predict the alloying effects on the WB_S temperatures of commercial steels by neglecting the effects of all alloying elements except for their thermodynamic effect on the calculation of driving force. However, they then observed the stronger effects of Cr and Mo and introduced linear coefficients for them. Figures 9 and 10 confirm the large and positive effects of Cr and Mo. Si appears to have a similar effect but, if evaluated per atom fraction, it would be smaller, in particular relative to Mo. One may wonder if the special effect of Mn and Ni is coupled to their strong stabilizing effect on austenite.

All the WB_S lines in Figures 7, 8, 9, 10, and 11 end inside the diagram when the carbon content, being a dependent variable here, approaches zero. This was illustrated for DFN_{crit} already with the set of curves for constant carbon content for Fe-C-Mn alloys in Figure 2. Similar curves for equal carbon content could have been included in Figures 7, 8, 9, 10, and 11 but the line for zero carbon can directly be imagined through the end points. In this sense, diagrams for both kinds of critical driving force have the same characteristic feature but one difference should be emphasized. For DFD_{crit} all the WB_S curves for equal alloy content in Figures 7, 8, 9, 10, and 11 demonstrate a strong increase with decreasing temperature but in Figure 2 for DFN_{crit} they decrease.

The strong temperature dependence of the critical driving force for a diffusional process appears to be closely related to the stability of ferrite as illustrated by the fact that the WB^o_S curve for binary Fe-C alloys has the same general shape as the well-known difference in molar Gibbs energy between austenitic and ferritic iron.[21] Both have fairly straight pieces separated by a range with obvious curvature between about 873 K and 923 K (600 °C and 750 °C), which is caused by the ferromagnetic transition of Fe-rich ferrite. This similarity was emphasized already by Hillert *et al.*[13] and indicates that the two curves are somehow related. It should be emphasized that the empirical Eq. [2] and Figure 1 give no indication of such a change with temperature. This kind of diagram does not appear to give any clue to what factor is governing the critical condition of bainite formation.

Due to the strong thermodynamic effect on the shape of $DFD_{crit}(T,0)$, it would not be possible to represent the W_S and B_S information with linear equations of the $DFD_{crit}(T,M)$ function such as the $T_{crit}(C,M)$ function in Eq. [2]. It could be mentioned that Bhadeshia[14] was able to use a straight line because he did not consider the W_S information in the high temperature range where the WB^o_S line deviates strongly from a straight line. Hillert *et al.*,[13] who obtained a curve similar to the WB^o_S curve in Figures 7, 8, 9, 10, and 11, described it analytically with a spline function, which they could use as a reference for estimates of the alloying effects of Cr and Mo on the B_S temperature. In the present work it will not be necessary to describe the $DFD_{crit}(T,M)$ function analytically because the same information is already available as $T_{crit}(C,M)$ through Eq. [2]. With an analytical expression of a WB_S line as a function of a critical driving force, B_S temperatures can be predicted, but the results would be identical to those obtained directly from Eq. [2] if the analytical expression had been derived from it. In general, the driving forces would not be of much use for predictions if they have been derived from an empirical equation already available. On the other hand, it may seem possible that WB_S information could give a clue about the physical nature of the transformation mechanism if it is expressed through a kind of critical driving force. This may help to construct a physically based model that could replace empirical ones.

V. USE OF CARBON CONTENT AS THE INDEPENDENT VARIABLE

As already mentioned, when Bhadeshia considered transformation stresses as an energy barrier for growth, he suggested a constant energy requirement of 400 J/mol independent of temperature, alloying element and carbon content. This seems like a very attractive model as an explanation of the critical condition for bainite formation. However, he coupled it to a diffusionless process, and in Section III it was found that empirical WB_S^o temperatures for binary Fe-C alloys occur at temperatures where the driving force for a diffusionless process is negative, which could not be accepted. It was then decided to try to couple the idea of an energy barrier to diffusion of carbon. However, to describe how the B_S temperature decreases with increasing carbon content, it would then be necessary to postulate that the height of the barrier increases with increasing carbon content. The $WB_S^o \equiv DFD_{crit}(C,0)$ function will now be explored, *i.e.*, the carbon content will be used as the independent variable. For simplicity, it will be assumed that the barrier in each alloy is independent of temperature and will be surmounted at a critical temperature on cooling when the driving force has grown to the magnitude of the barrier. Already when starting from the basic function in Eq. [2], which was based on the $WB_S \equiv T_{crit}(C,M)$ function, it may seem convenient also to regard the energy barrier as a function of the carbon content, C.

The DFD_{crit} quantities plotted as $WB_S \equiv DFD_{crit}(T,Mn)$ in Figure 7 were then plotted as $WB_S \equiv DFD_{crit}(C,Mn)$ in Figure 12, but isotherms were included to illustrate how the narrow group of lines for various Mn contents in Figure 7 is now well separated because of differences in carbon content but falls at almost constant temperature. The seemingly interesting variation of the effect of Mn, illustrated in the insert of Figure 7, now appears to be a trivial effect of a slight curvature of the isotherms in Figure 12. The small effects of Mn and Ni in Figures 7 and 8, compared with the larger effects of Mo, Cr and Si in Figures 9, 10, and 11, seem to be directly related to the small slope of isotherms in this kind of diagram.

Figures 13, 14, 15, and 16 show the remaining ternary systems with parallel WB_S lines for up to 10 mass pct alloying element. All have positive slopes and show that, for constant alloy content, DFD_{crit} increases with increasing carbon content. The effect of the alloy content is smaller for Ni and slightly larger for Mo than for the others, which have about equal effects. Expressed per atom fraction, the effect of Si will be smaller and that of Mo larger.

The WB_S^o line for binary Fe-C alloys is included as a dashed line in Figures 12, 13, 14, 15, and 16. It exhibits a curvature below 1.2 mass pct carbon and has about the same shape as in Figures 7, 8, 9, 10, and 11 where it was plotted *vs* T instead of C. Since this feature was explained as a thermodynamic effect on the shape of the $WB_S^o \equiv DFD_{crit}(T,0)$ function in Section IV, it would seem that the same effect has influenced the shape of the $WB_S^o \equiv DFD_{crit}(C,0)$ function in Figures 12, 13, 14, 15, and 16. The curved parts vanish gradually with increasing alloy content in both sets of figures, which seems natural when T is used as the independent variable in Figures 7, 8, 9, 10, and 11 because a piece of the high temperature end of the WB_S line is cut off for each addition of alloying element and that is where the ferromagnetic transition of Fe-rich ferrite causes the WB_S line to curve. It also happens when C is used as the independent variable in Figures 12, 13, 14, 15, and 16 but there it may seem less natural. However, the isotherms in Figure 12 reveal that it is again the high temperature parts of the WB_S lines that are being cut off. The carbon dependence of $DFD_{crit}(C,M_1)$ is rather linear from 3 mass pct alloy element.

Considering the shape of the $WB_S^o \equiv DFD_{crit}(C,0)$ curve in Figures 12, 13, 14, 15, and 16, it may be suggested that it formally describes an energy barrier that increases with the carbon content because of some interaction between carbon atoms and the phase interface. Furthermore, DFD_{crit} in Figures 12, 13, 14, 15, and

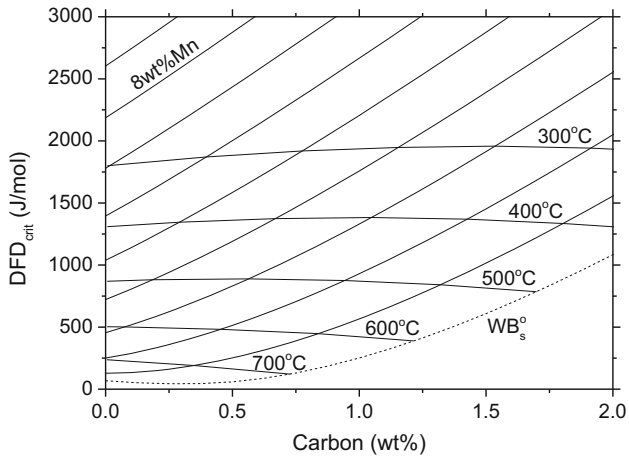

Fig. 12—Critical driving force for a diffusional process as a function of carbon content for Fe-C-Mn up to 9 wt pct Mn shown together with intersecting horizontal isotherms from 300 °C to 700 °C.

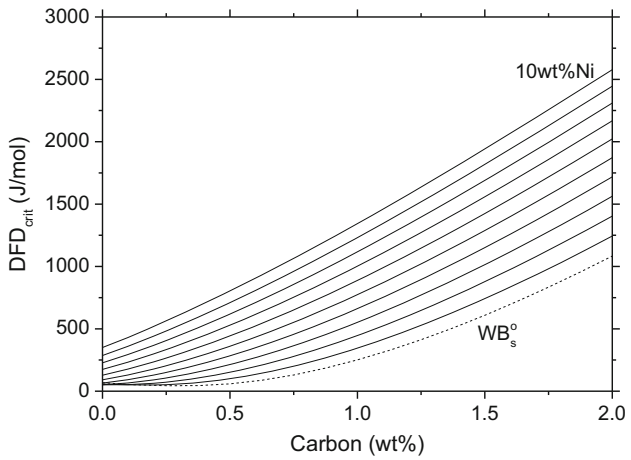

Fig. 13—Critical driving force for a diffusional process as a function of carbon content for Fe-C-Ni up to 10 wt pct Ni.

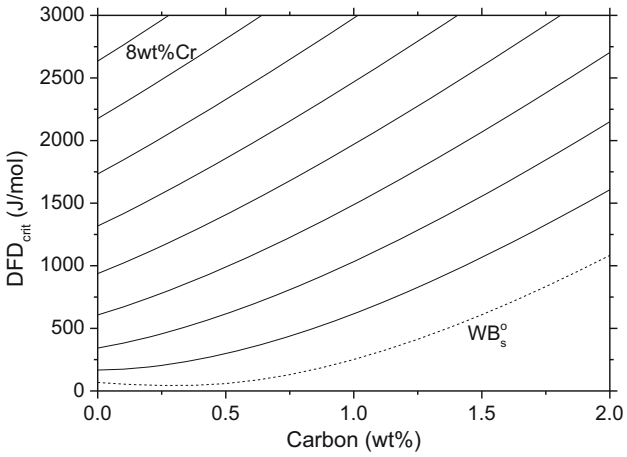

Fig. 14—Critical driving force for a diffusional process as a function of carbon content for Fe-C-Cr up to 8 wt pct Cr.

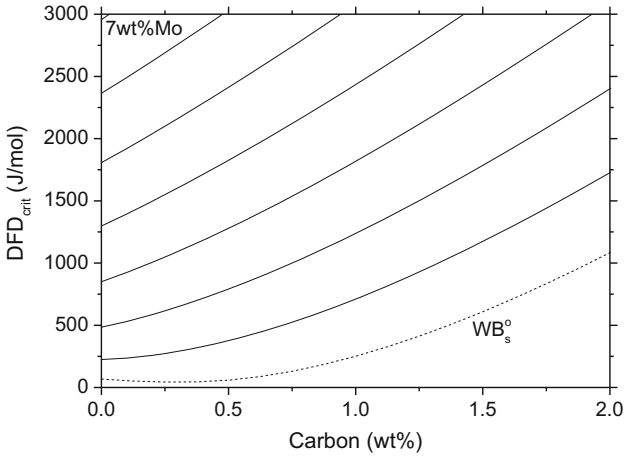

Fig. 15—Critical driving force for a diffusional process as a function of carbon content for Fe-C-Mo up to 7 wt pct Mo.

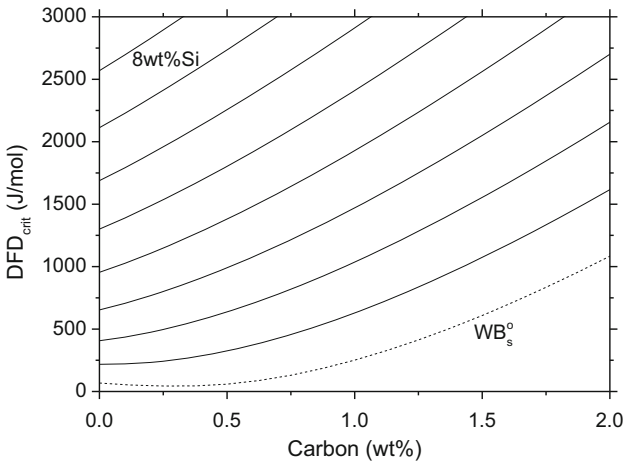

Fig. 16—Critical driving force for a diffusional process as a function of carbon content for Fe-C-Si up to 8 wt pct Si.

16 increases with all the investigated alloying elements. It is evident that their contribution to the energy barrier is predicted to be roughly proportional to the alloy content and independent of the carbon content. It may thus have a different origin. On the other hand, it should be realized that these characteristic features have been imposed upon the $WB_S \equiv DFD_{crit}(C, M)$ function by the use of linear terms in Eq. [2]. This has been applied almost universally to empirical equations of the effect of composition on the B_S temperature. It may not be justified to try to interpret this predicted effect of alloying elements until the possible interaction between carbon and alloying elements has been subjected to a closer study. In particular, it should be emphasized that the extension to low carbon contents of all the WB_S lines in Figures 12, 13, 14, 15, and 16 are based on extrapolations from experimental information at higher carbon contents. As an example, it might be interesting to make the terms for alloying elements proportional to both the carbon and alloy content.

VI. DERIVATION OF AN ANALYTICAL EXPRESSION

As mentioned, predictions of critical temperatures from a critical driving force as a function of composition will give results identical to those obtained from the primary empirical Eq. [2] from which the critical driving force was derived. However, there may be particular applications requiring an analytical expression for rapid calculations of the critical driving force for a diffusional process from the composition of steels and without continuous access to thermodynamic software and database, which is what Eq. [2] can do for the critical temperature. For this purpose, an analytical equation will now be derived for the $WB_S \equiv DFD_{crit}(C, M_1)$ function by fitting of coefficients to the lines in Figures 12, 13, 14, 15, and 16. The following analytical expression was found to give sufficient results.

$$DFD_{crit} = A_C + B_C u_C + C_C u_C^2 + \sum_i \left(A_{M_i} u_C u_{M_i} + B_{M_i} u_{M_i} + C_{M_i} u_{M_i}^2 \right), \quad [9]$$

where u_i ($i = C,M$) is a composition variable defined in connection to Eq. [6]. $A_C, B_C$and C_C are coefficients for carbon, and A_M, B_MandC_M are those for a given alloy system. The function was first fitted to the WB_S^o line to evaluate the coefficients for carbon, which will represent the barrier for binary Fe-C alloys. The remaining coefficients were evaluated for one alloying element at a time by fitting to the WB_S lines in the ternary Fe-C-M diagrams. The result is presented in Table I and Figures 17, 18, 19, 20, and 21. Due to the choice of an expression without temperature as an independent variable, the result will represent an energy barrier that is independent of temperature but is equal to the

Table I. Coefficients in Eq. [9]

Alloy element	A (J/mol)	B (J/mol)	C (J/mol)
C	70	− 4560	178,900
Cr	460,000	7200	300,000
Mn	482,000	3600	300,000
Mo	744,000	31,500	890,000
Ni	219,000	− 1600	46,000
Si	221,000	6550	68,600

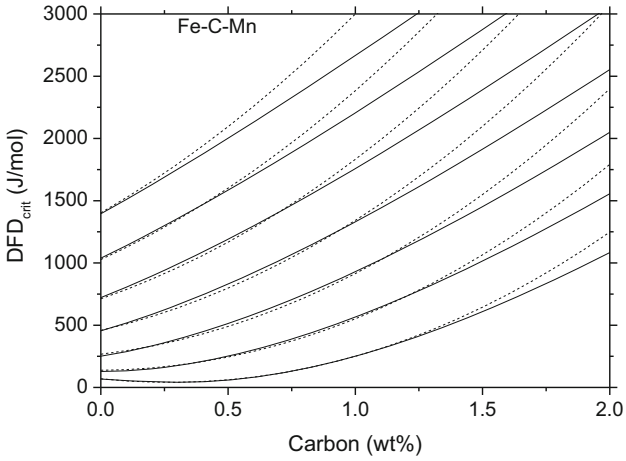

Fig. 17—Critical driving force for a diffusional process plotted with carbon content for Fe-C-Mn up to 6 wt pct Mn. Solid lines are calculated from Eq. [2], and dashed lines are calculated from Eq. [9].

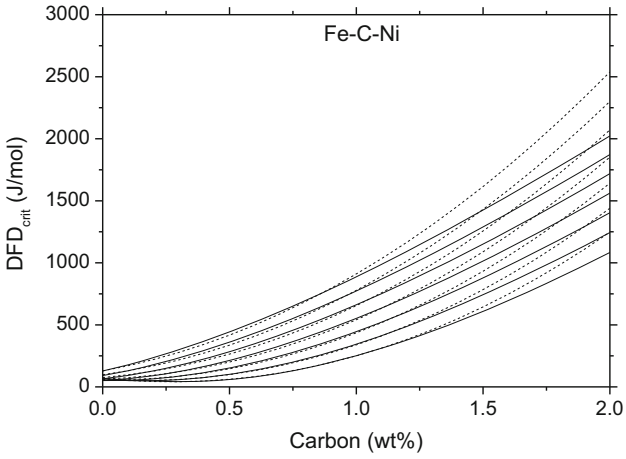

Fig. 18—Critical driving force for a diffusional process plotted with carbon content for Fe-C-Ni up to 6 wt pct Ni. Solid lines are calculated from Eq. [2], and dashed lines are calculated from Eq. [9].

available driving force only at a particular temperature for each alloy, its B_S temperature.

The chosen shape of Eq. [9] was primarily based on a decision to use the least number of fitting parameters for achieving sufficient fit. Figures 17, 18, 19, 20, and 21 show how the function of Eq. [9] (dashed lines) compares with the function of Eq. [2] (solid lines). At low carbon contents, the difference is negligible but

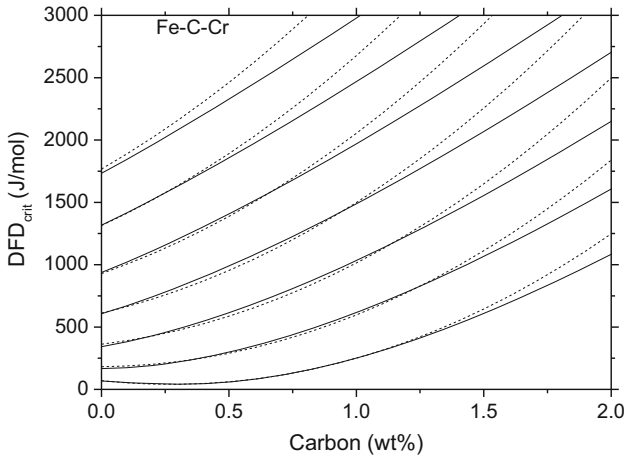

Fig. 19—Critical driving force for a diffusional process plotted with carbon content for Fe-C-Cr up to 6 wt pct Cr. Solid lines are calculated from Eq. [2], and dashed lines are calculated from Eq. [9].

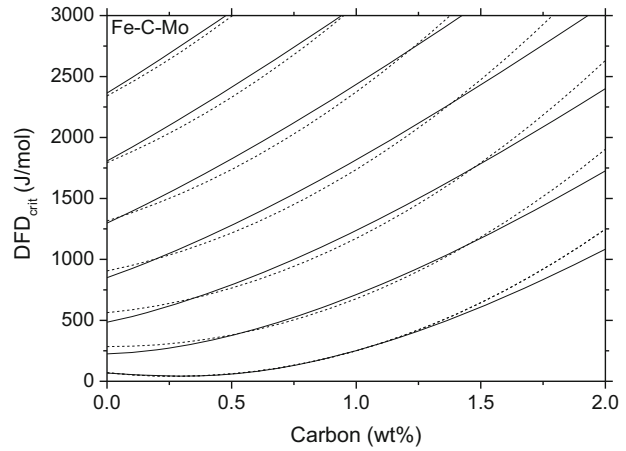

Fig. 20—Critical driving force for a diffusional process plotted with carbon content for Fe-C-Mo up to 6 wt pct Mo. Solid lines are calculated from Eq. [2], and dashed lines are calculated from Eq. [9].

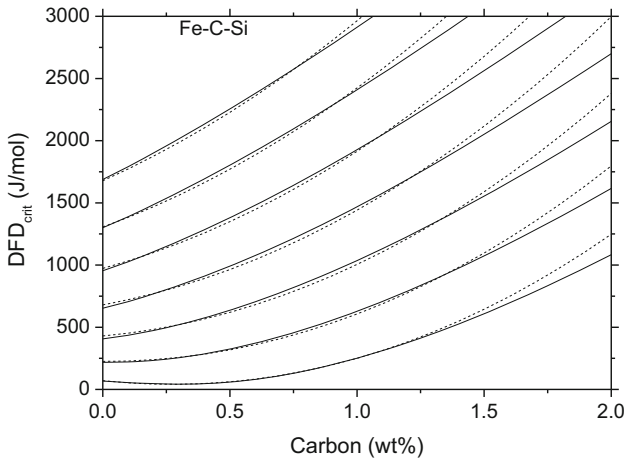

Fig. 21—Critical driving force for a diffusional process plotted with carbon content for Fe-C-Si up to 6 wt pct Si. Solid lines are calculated from Eq. [2], and dashed lines are calculated from Eq. [9].

becomes more considerable as the amount of alloying element increases as can be seen from the 6 mass pct line for Cr in Figure 20. The use of the function should thus be limited to 4 mass pct Mn and Cr though 6 mass pct may be permissible for Ni, Mo and Si.

The accuracy of Eq. [9] relative to Eq. [2], which is the link to the experimental information, was tested by comparing the WB_S temperatures, calculated using Eq. [9] with experimental temperatures taken from a similar test of Eq. [2], which was performed in Reference 11. As expected, the present results looked very similar but the root mean square (RMS) of differences had slightly increased from 70 K to 77 K for one group of data and from 76 K to 80 K for another group. The difference is expected in view of the fitting not being perfect as seen in Figures 17, 18, 19, 20, and 21. For further information on the experimental data the reader is referred to Reference 11. It was concluded that Eq. [9] can be used for predicting bainite start temperatures from the composition of an alloy by first calculating DFD_{crit} from Eq. [9] and then finding the corresponding temperature in the function $DFD(T)$ for the same composition. However, it should be realized that the same prediction can be made from Eq. [2], which was evident from the test just described. The new equation could possibly be of more practical use if it is modified by direct fitting to the primary experimental information.

VII. SUMMARY AND CONCLUSIONS

The present work was based on the following premises. The start temperature of bainite in an alloy with fixed composition is regarded as a critical temperature, T_{crit}. For alloys with equal alloy content, T_{crit} may vary with the carbon content, here abbreviated with C, *i.e.*, as $T_{crit}(C)$. This function can be presented as a line in a T,C diagram, the B_S line for the respective alloy content. One may thus represent a B_S line with this function and express B_S as $T_{crit}(C)$, which was done in Eq. [1]. The same B_S line can also be expressed with the $C_{crit}(T)$ function.

Various processes related to the formation of bainite can possibly be imagined, and, with a thermodynamic database, the driving force for any such process can be calculated as a function of temperature, $DF(T)$. It is assumed that the process can proceed only if it surmounts an energy barrier of a height, H, and that will occur at a critical temperature for each alloy or a critical carbon content at fixed alloy content and temperature. The driving force will then have a critical value, $DF_{crit} = H$, where DF_{crit} can be obtained as either $DF_{crit}(T)$ or $DF_{crit}(C)$. Once a B_S line has been defined as any of the above functions, all the other functions can be calculated with a proper database.

The empirical Eq. [2] for B_S information was used as a source of information for the present study of the critical driving force for the start of bainite formation. Equation [2] was derived with attention to information from binary Fe-C alloys including Widmanstätten ferrite as well as bainite. It is thus possible to use it with some confidence in calculations of driving forces for binary Fe-C alloys, which include Widmanstätten ferrite. The B_S lines in diagrams for constant alloy contents were therefore denoted as WB_S and the line for binary Fe-C alloys was denoted as WB_S^o. These notations were applied independent of the axis variables, and the WB_S quantity is thus expressed in units of temperature, carbon content or driving force. A WB_S line can appear in several diagrams with different sets of axes but still representing the same series of critical conditions for bainite formation.

In the present work, critical driving forces were calculated for WB_S lines obtained from the empirical Eq. [2]. Negative values for the critical driving force of a diffusionless process were obtained for binary Fe-C alloys. It is thus concluded that bainitic ferrite cannot form by a completely diffusionless process. It seems that Bhadeshia's model of an energy barrier, caused by transformation stresses, cannot be combined with a diffusionless process. The accuracy of the empirical information may be questioned, in particular for binary Fe-C alloys. However, considering an appreciable number of similar empirical equations, derived in different ways, it seems unlikely that future revision will modify the calculated critical driving forces for a diffusionless process enough to yield positive driving forces in binary Fe-C alloys.

The critical driving force for a diffusional process in binary Fe-C alloys was first calculated and plotted *vs* temperature. The strong temperature dependence, observed previously, was confirmed. It may be closely related to the temperature dependence of the Gibbs energy difference between austenitic and ferritic Fe though it does not seem to give a clue as to the nature of the physical effect governing the critical condition. The shape of the critical driving force for binary Fe-C alloys was then plotted*vs* carbon content and the $WB_S^o \equiv DFD_{crit}(C,0)$ function was regarded as an energy barrier for bainite formation caused by carbon because it increased with the carbon content. However, it seems to have some feature related to thermodynamic properties of iron.

The effects of alloying elements on the critical driving force of a diffusional process were very small for Mn and Ni when plotted *vs* temperature but more similar to the effects of other elements when plotted *vs* carbon content. One can thus neglect these elements in predictions of B_S temperatures from the $WB_S \equiv DFD_{crit}(C,M_1)$ function but not from the $WB_S \equiv DFD_{crit}(C,M_1)$ function. The effects of alloying elements in empirical equations have not been evaluated as functions of carbon content, and the empirical equations that are presently available should not be extrapolated to low carbon contents.

How the $WB_S \equiv DFD_{crit}(C,M_1)$, function, derived from an empirical equation for B_S temperatures, can be presented analytically was demonstrated, and it can be used for predicting the start of bainite formation but would be particularly useful for calculating the critical driving force for a diffusional process without access to a thermodynamic database. In future work, this equation could be improved by determining its coefficients with direct fitting to improved experimental values and paying special attention to the coefficients controlling the assumed energy barrier for binary Fe-C alloys. One should consider the possibility of making the alloy

contributions dependent on the carbon content. Improved experimental information is badly needed on binary Fe-C alloys and ternary alloys in a range of low carbon contents.

ACKNOWLEDGMENTS

This study was conducted within the VINN Excellence Center Hero-m and Competence Center Hero-m2 Innovation. The authors acknowledge the financial support provided by VINNOVA, the Swedish Governmental Agency for Innovation Systems, Swedish Industry and KTH Royal Institute of Technology.

OPEN ACCESS

REFERENCES

1. W. Steven and A.G. Haynes: *J. Iron Steel Inst*., 1956, vol. 183, pp. 349–59.
2. J.S. Kirkaldy and G. Venugopalan: in *Phase Transformations in Ferrous Alloys*, A.R. Marder and J.I. Goldstein, eds., TMS AIME, Warrendale, 1984.
3. M. Suehiro, T. Senuma, H. Yada, Y. Matsumura, and T. Ariyoshi: *Tetsu-to-Hagané*, 1987, vol. 73, pp. 1026–33.
4. R.L. Bodnar, T. Ohashi, and R.I. Jaffee: *Metall. Trans. A*, 1989, vol. 20A, pp. 1445–60.
5. J. Zhao and Z. Jin: *Mater. Sci. Techn*., 1992, vol. 8, pp. 1004–10.
6. T. Kunitake and Y. Okada: *J. Iron Steel Jpn*., 1998, vol. 84, pp. 137–41.
7. J. K. Lee: *Prediction of Tensile Deformation Behavior of Formable Hot Rolled steels*. POSCO Technical Resrearch Laboratoreis Report, POSCO, Pohang, (1999).
8. J. Zhao, C. Liu, Y. Liu, and D.O. Northwood: *J. Mater. Sci*., 2001, vol. 36, pp. 5045–56.
9. Y.K. Lee: *J. Mater. Sci*., 2002, vol. 21, pp. 1253–55.
10. S.M.C. van Bohemen: *Mater. Sci. Technol*., 2012, vol. 28, pp. 487–95.
11. L. Leach, P. Kolmskog, A. Borgenstam, L. Höglund and M. Hillert: *Empirical methods to predict bainite start conditions*. Unpublished work.
12. M. Hillert: *The growth of ferrite, bainite and martensite,* Report, Swedish Inst. Metal Research, 1960. Printed in Thermodynamics and Phase Transformations, The Selected Works of Mats Hillert. Eds. J. Ågren, Y. Bréchet, C. Hutchinson, J. Philibert and G. Purdy, EDP Science,Les Ulis Cedex, 2006.
13. M. Hillert, L. Höglund, and J. Ågren: *Metall. Mater. Trans*., 2004, vol. 35A, pp. 3693–3700.
14. H.K.D.H. Bhadeshia: *Acta Metall*., 1981, vol. 29, pp. 1117–30.
15. A. Hultgren: *Trans. ASM*, 1947, vol. 39, pp. 915–89.
16. J.O. Andersson, T. Helander, L. Höglund, P. Shi, and B. Sundman: *Calphad*, 2002, vol. 26, pp. 273–312.
17. *TCFE8-TCS Steels/Fe-Alloys Database,* v8. 0.2015.
18. H.K.D.H. Bhadeshia: *Metal Sci*., 1982, vol. 16, pp. 159–65.
19. M. Peet and H.K.D.H Bhadeshia: www.phase-trans.msm.cam.ac.uk.
20. H.K.D.H. Bhadeshia and D.V. Edmonds: *Metall. Trans. A*, 1989, vol. 20A, pp. 330–32.
21. H.L. Lukas, S.G. Fries, and B. Sundman: *Computational Thermodynamics. The Calphad Method*, Cambridge University Press, Cambridge, 2007.